For Case III using 32-QAM and 64-QAM, based on the adaptive power loading procedure described in [4], the effectiveness of adaptive power loading in combating the system frequency response roll-off effect is examined in Fig. 3, where the loaded subcarrier power distributions in the transmitter are presented together with the received subcarrier power distributions in the receiver, all of which are normalized to the power of the corresponding first subcarrier. As expected, Fig. 3 indicates that adaptive power loading can efficiently compensate for the VCSEL-based IMDD OOFDM system frequency response roll-off effect. It should be pointed out that the differences of the loaded/received subcarrier powers between the 32-QAM and 64-QAM cases in Fig. 3 are due to the fact that a lower signal modulation format is more tolerant to the quantization effect at low signal amplitudes. This reduces the minimum allowed subcarrier amplitude, thus leading to an increased amplitude dynamic range.

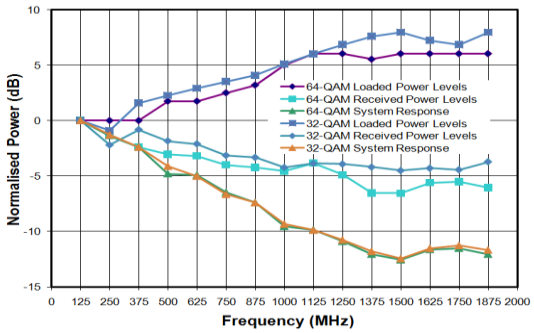

Fig. 3. Loaded/received subcarrier power levels and system frequency response for Case III using 32-QAM and 64-QAM.

To further verify the above statement, the 64-QAM-encoded OOFDM signal spectra at the output of the VCSEL intensity modulator with equal power loading and adaptive power loading are compared in Fig. 4. It can be seen in Fig. 4 that, for the case of utilizing equal power loading, a sharp decay of the OOFDM signal spectrum occurs. On the contrary, adaptive power loading gives rise to a relatively flat OOFDM signal spectrum.

Under the optimum loaded subcarrier power profiles presented in Fig. 3, the measured subcarrier error distributions are shown in Fig. 5 for Case III. It can be seen in Fig. 5 that adaptive power loading enables almost uniform subcarrier error distributions with a less than ± 12.5% (± 6%) variation for 64-QAM (32-QAM). This confirms, once again, that the adaptive power loading technique can effectively compensate for the system frequency response roll-off effect, thus resulting in an acceptable total channel BER obtained, as discussed in Subsection 3.2. The occurrence of the highest error peak corresponding to the 15th subcarrier in Fig. 5 is mainly due to the following two physical mechanisms: (1) the residual received power roll-off effect induced by the finite dynamic subcarrier power variation range, as shown in Fig. 3; (2) imperfect subcarrier orthogonality-induced inter-channel interference (ICI). Imperfect orthogonality between different subcarriers within a symbol arises due to the quasi-periodic structure of time domain OFDM symbols. Such an error peak can be considerably reduced when the signal extinction ratio of the OOFDM signal is increased [15].

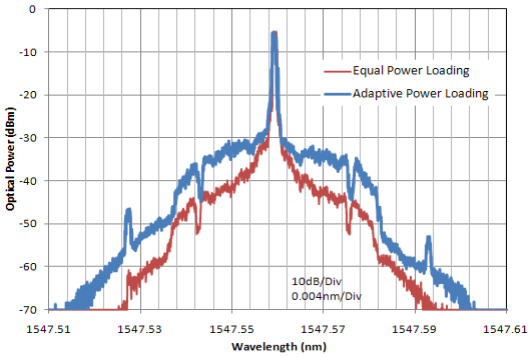

Fig. 4. Real-time 64-QAM-encoded OOFDM signal spectra at the output of the VCSEL intensity modulator with equal power loading and adaptive power loading.

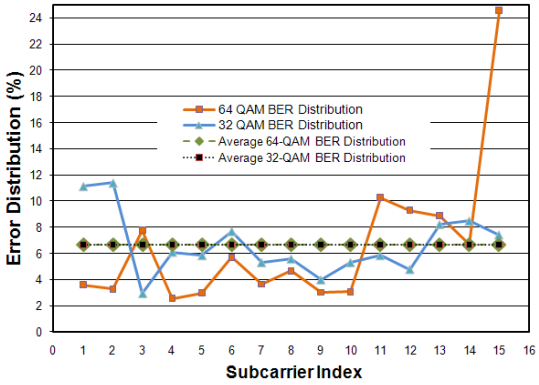

Fig. 5. Typical subcarrier error distribution for 32-QAM and 64-QAM over 25km SSMF when adaptive power loading is used.

3.2 Total channel BER performance

Based on the optimum loaded subcarrier power profiles, end-to-end real-time transmission of 11.25Gb/s (9.375Gb/s) 64-QAM- (32-QAM)-encoded OOFDM signals is experimentally demonstrated over 25km SSMF IMDD PON systems involving VCSEL intensity modulators. Figure 6 shows the measured total channel BER performance for both Case II and Case III.

From Fig. 6, it is observed that, for 11.25Gb/s 64-QAM-encoded OOFDM signals, the total channel BERs of 1.1×10^{-3} and 1.2×10^{-3} are obtainable for Case II and Case III, respectively. The corresponding power penalty at a FEC limit of 4×10^{-3} [16] is approximately 0.5dB. Whilst for 9.375Gb/s 32-QAM-encoded OOFDM signals, the total channel BERs as low as 5.2×10^{-5} and 6.9×10^{-5} are feasible for Case II and Case III, respectively, with a negligible power penalty at the above-mentioned FEC limit. Such substantial improvement in system BER performance for a lower signal modulation format indicates that the dynamic system frequency response roll-off effect does not considerably affect the system performance due to the use of adaptive power loading. The main physical factor determining the minimum achievable BER is the relatively low extinction ratio of the VCSEL intensity-modulated OOFDM signal [15]. Generally speaking, a small signal extinction ratio reduces the effective signal-to-noise ratio (SNR) of a received OOFDM signal for a specific photon detector. Therefore, an OOFDM signal encoded using a high signal modulation format is more susceptible to the effective SNR reduction, compared to an OOFDM signal encoded using a low signal modulation format. This is the physical mechanism underpinning the BER difference between the 64-QAM and 32-QAM cases, as shown in Fig. 6. In addition, the error-floor like BER performance observed in Fig. 6 is a

#139519 - $15.00 USD Received 13 Dec 2010; revised 28 Jan 2011; accepted 28 Jan 2011; published 1 Feb 2011

result of the low signal extinction ratio-induced small effective SNR of the received OOFDM signal.

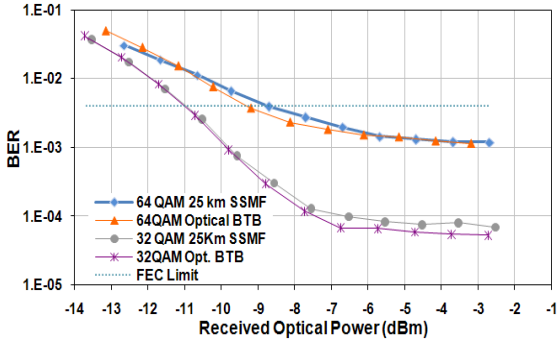

Fig. 6. BER performance for optical back-to-back and transmission over 25km SSMFs for 32-QAM and 64-QAM modulation formats.

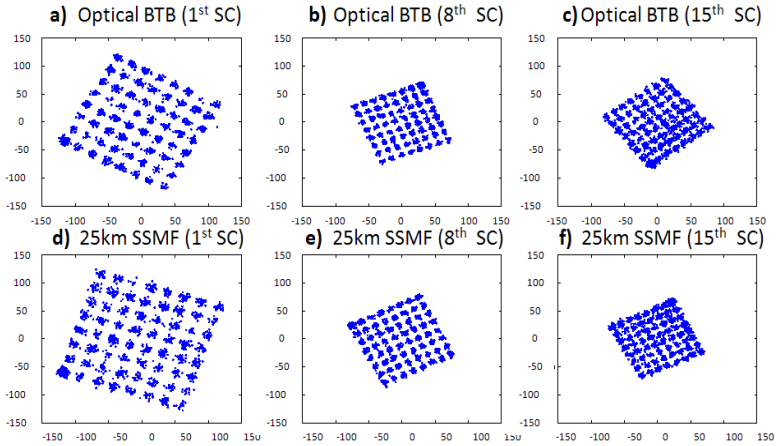

Fig. 7. Received 64-QAM constellations of individual subcarriers before equalization. Optical back-to-back, total channel BER = 1.1×10^{-3} (a, b, c) 25km SSMF, total channel BER = 1.2×10^{-3}, (d, e, f).

Representative constellations of individual subcarriers of the 11.25Gb/s 64-QAM-(9.375Gb/s 32-QAM)-encoded OOFDM signals corresponding to the total channel BERs of 1.1×10^{-3} for Case II and 1.2×10^{-3} for Case III (5.2×10^{-5} for Case II and 6.9×10^{-5} for Case III) are presented in Fig. 7 (Fig. 8). These constellations are recorded prior to performing channel equalization in the receiver. All the constellations show a variation in amplitude level corresponding to the power variation shown in Fig. 3. In comparison with their optical back-to-back counterparts, the constellations for Case III show very little deviations. This is reflected in the small BER difference between these two cases, as shown in Fig. 6.

#139519 - $15.00 USD Received 13 Dec 2010; revised 28 Jan 2011; accepted 28 Jan 2011; published 1 Feb 2011

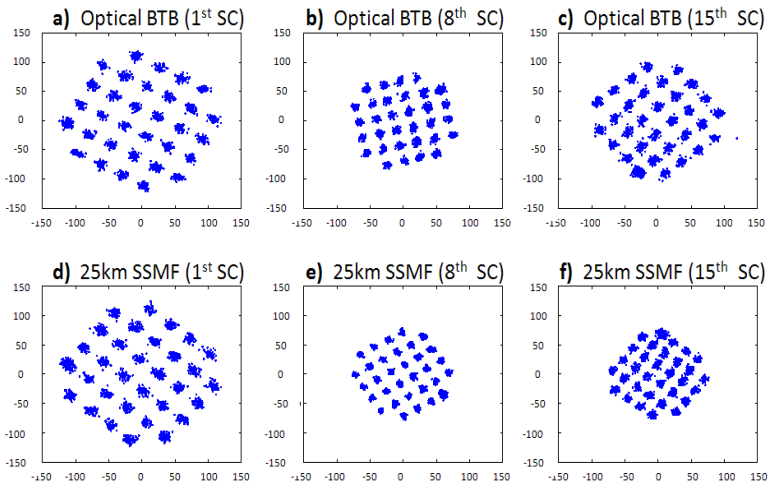

Fig. 8. Received 32-QAM constellations of individual subcarriers before equalization. Optical back-to-back, total channel BER = 5.2×10^{-5} (a, b, c) 25km SSMF, total channel BER = 6.9×10^{-5} (d, e, f).

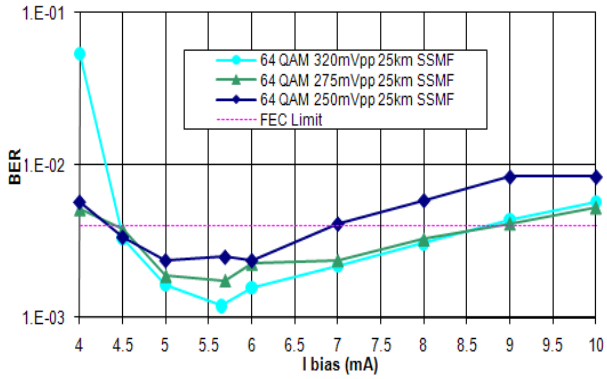

Fig. 9. Bias and driving current dependent total channel BER performance.

3.3 System performance robustness

As a large dynamic operating condition range of the adopted intensity modulator can significantly improve the system performance robustness, from the practical system design point of view, it is greatly advantageous if the VCSEL intensity modulator can operate over a wide range of DC bias currents and driving voltages, without considerably compromising the system performance compared to that obtained under the identified optimum intensity modulator operating conditions. In this subsection, we show experimentally that, apart from the considerable improvement in transmission performance, adaptive power loading can also significantly extend the VCSEL dynamic operating condition range, due to its capability of compensating for the dependence of the system frequency response upon variations in DC bias current and driving voltage.

Figure 9 shows the total channel BER performance as a function of DC bias current and driving voltage for Case III using 64-QAM. In obtaining this figure, the DC bias current varies in a range of 4mA to 10mA, as the VCSEL's lasing threshold is 2mA and the absolute maximum forward current specified by the manufacturer is 15mA. In addition, the applied driving voltage also varies within a large range of 250mVpp to 320mVpp. In the experimental measurements, live adjustment of the loaded subcarrier power profiles is performed for each

#139519 - $15.00 USD Received 13 Dec 2010; revised 28 Jan 2011; accepted 28 Jan 2011; published 1 Feb 2011

of the selected DC bias currents and/or driving voltages. It should also be noted, in particular, that no VCSEL dynamic operating range exists for equal power loading, as equal power loading does not enable the present transmission system to operate under the FEC limit even when the identified optimum VCSEL operating conditions are adopted.

It is very interesting to note in Fig. 9 that total channel BERs below the FEC limit are obtainable for bias currents ranging from 4.5mA to 9mA and driving voltages ranging from 275mVpp to 320mVpp. A 2mA reduction of the aforementioned bias current range, i.e., from 9mA to 7mA, decreases the minimum allowed driving voltage to a value as low as 250mVpp, thus broadening the driving voltage range by 25mVpp. For DC bias currents of less than the optimum value of 5.57mA, the BER reduction with increasing bias current is mainly due to the reduced signal clipping effect, because a smaller portion of the lower part of the driving signal penetrates into the region below the VCSEL lasing threshold. On the other hand, for DC bias currents of higher than the optimum value of 5.57mA, the BER increase with increasing bias current is mainly due to the large DC component-induced reduction in signal extinction ratio: a low signal extinction ratio increases OOFDM signal susceptibility to noise [15]. Moreover, Fig. 9 also shows that, for a given bias current, an increase in driving voltage decreases the total channel BER over almost the entire bias current and driving voltage regions. This suggests, once again, that, in comparison with the VCSEL frequency chirp effect, a low extinction ratio of the VCSEL intensity-modulated OOFDM signal is a dominant factor limiting the performance of the current transmission system.

4. Conclusions

The feasibility of utilising low-cost, un-cooled VCSELs as intensity modulators in previously demonstrated real-time OOFDM transceivers has been extensively explored experimentally, for the first time, in terms of achievable signal bit rates, physical mechanisms limiting the transceiver performance and performance robustness. Making use of such transceivers, end-to-end real-time transmission of 11.25Gb/s 64-QAM-encoded OOFDM signals over 25km SSMF IMDD PON systems has been experimentally demonstrated with a power penalty of 0.5dB. It has been identified that a low extinction ratio of the VCSEL intensity-modulated OOFDM signal is the dominant factor determining the maximum obtainable system performance. Experimental investigations have also indicated that, in addition to the enhanced transceiver performance, adaptive power loading can significantly improve the system performance robustness to variations in VCSEL operating conditions. As a direct result, the aforementioned capacity versus reach performance is still retained over a wide VCSEL bias current (driving voltage) range of 4.5mA to 9mA (275mVpp to 320mVpp). Given the fact that conventional DFB lasers take the majority of the OOFDM transceiver cost, this work is of great value as it demonstrates the possibility of future mass production of cost-effective OOFDM transceivers for PON applications. In addition, the utilisation of large modulation bandwidth (>10GHz) and highly linear VCSELs with steep L-I curves in the OOFDM systems could increase the VCSEL-based OOFDM transceiver speeds to 40Gb/s. Such VCSELs are becoming commercially available and have the potential for achieving low cost when mass produced.

Acknowledgements

This work was partly supported by the EC's Seventh Framework Programme (FP7/2007-2013) within the project ICT ALPHA under grant agreement n° 212 352, and in part by the Welsh Assembly Government and The European Regional Development fund. The authors would also like to thank APEX technologies for the loan of the optical spectral analyser (AP2440A).

#139519 - $15.00 USD Received 13 Dec 2010; revised 28 Jan 2011; accepted 28 Jan 2011; published 1 Feb 2011